

Competitive Diels–Alder Reactions: Cyclopentadiene and Phospholes with Butadiene

T. C. Dinadayalane,[†] G. Gayatri,[‡] G. Narahari Sastry,^{*,‡} and Jerzy Leszczynski^{*,†}

Computational Center for Molecular Structure and Interactions, Department of Chemistry, Jackson State University, 1400 JR Lynch Street, P.O. Box 17910, Jackson, Mississippi 39217, and Molecular Modeling Group, Organic Chemical Sciences, Indian Institute of Chemical Technology, Hyderabad 500 007, India

Received: June 16, 2005; In Final Form: August 5, 2005

Diene–dienophile competing Diels–Alder reaction pathways of cyclopentadiene, 1*H*-, 2*H*- and 3*H*-phospholes with butadiene were explored at the B3LYP level using 6-31G(d) and 6-311+G(d,p) basis sets, and at the CCSD(T)/6-31G(d)//B3LYP/6-31G(d) level. Activation barriers show that cyclopentadiene favors a diene rather than a dienophile conformation. Pathways 1 and 2 (A and B) corresponding to butadiene as the diene and dienophile are predicted to be highly competitive in the case of 1*H*-phosphole. Secondary orbital interactions and the preferable bispericyclic nature of transition states are responsible for the stability of endo transition states. The study indicates that some of the transition states are bispericyclic and most of them are highly asynchronous. The reactions require a lower activation energy when the conversion of weak C=P to C–P occurs in the case of 2*H*- and 3*H*-phospholes. The high stability of the products resulting via path 1 can be attributed to the less strain in the bicyclo[4.3.0]nonadiene skeleton compared to the norbornene derivatives obtained from path 2. Activation and reaction energy values for these Diels–Alder reaction pathways are compared with the values reported for the [4+2] cyclodimerizations of each of the reactants to examine the likelihood of cyclodimerizations along these pathways.

Introduction

Cycloaddition reactions are versatile synthetic organic routes in obtaining complex molecular architectures and particularly, [4+2] Diels–Alder cycloaddition reactions have been indispensable tools for successful syntheses of novel molecular targets.^{1–5} Cycloaddition reactions of phospholes have been employed to access novel polycyclic organophosphorus compounds. Many of the phosphorus-containing cycloadducts have promising applications in the fields of homogeneous catalysis and molecular materials.^{6–15} [4+2] cycloaddition reactions of phospholes with various dienophiles have been the subject of both experimental^{6–15} and theoretical interest.^{16–23} The notable contribution of Mathey's group has received special attention in the chemistry of phospholes that includes the cycloaddition with a wide range of dienophiles, interconversion of phospholes through a [1,5] sigmatropic shift, cyclodimerizations, enhancing the reactivity of phospholes by different substituents, reactions with transition metal derivatives to give organometallic complexes and applications of compounds derived from phospholes.^{6–14}

The discovery of a parent phosphole has led to intense research interest on the structures and reactivities of phospholes.^{12,13} Mathey and co-workers have reported a facile dimerization of 2*H*-phosphole to yield an endo dimer containing a P–P bond as a major product,¹² which has been confirmed by the recent computational study.¹⁷ This 2*H*-phosphole dimer has been recently reported as the starting material for biphospholene, which shows potential as a chelating ligand for

asymmetric catalysis.⁹ Experimental studies have demonstrated that 2*H*-phospholes tend to undergo well-defined [4+2] Diels–Alder reactions as both the diene and dienophile.^{13,14} Mathey has shown the parallel between the chemistry of phospholes and cyclopentadiene.^{6,7} Diels–Alder reactions between 1*H*-phosphole and dienophiles yielded 1-phosphanorbornene skeletons that are actually products of 2*H*-phosphole. Mathey has suggested that 1*H*-phosphole undergoes a [1,5] sigmatropic shift to 2*H*-phosphole, which then is involved in the Diels–Alder reaction.¹³ Computational studies have validated this mechanistic proposal of Mathey.^{16,21} Aromaticity, [1,5] sigmatropic shifts and Diels–Alder reactions of phospholes with different dienophiles have been studied theoretically.^{16–24} Two of us have recently reported all the possible [4+2] cyclodimerizations of phospholes and the propensity for further reactivities of dimers.¹⁷ Bachrach and Perriott have examined the reactions of butadiene with 2*H*-phosphole as both the diene and dienophile,²³ and these types of reactions are interesting as well as challenging to study computationally due to the possibility of competitive pathways.

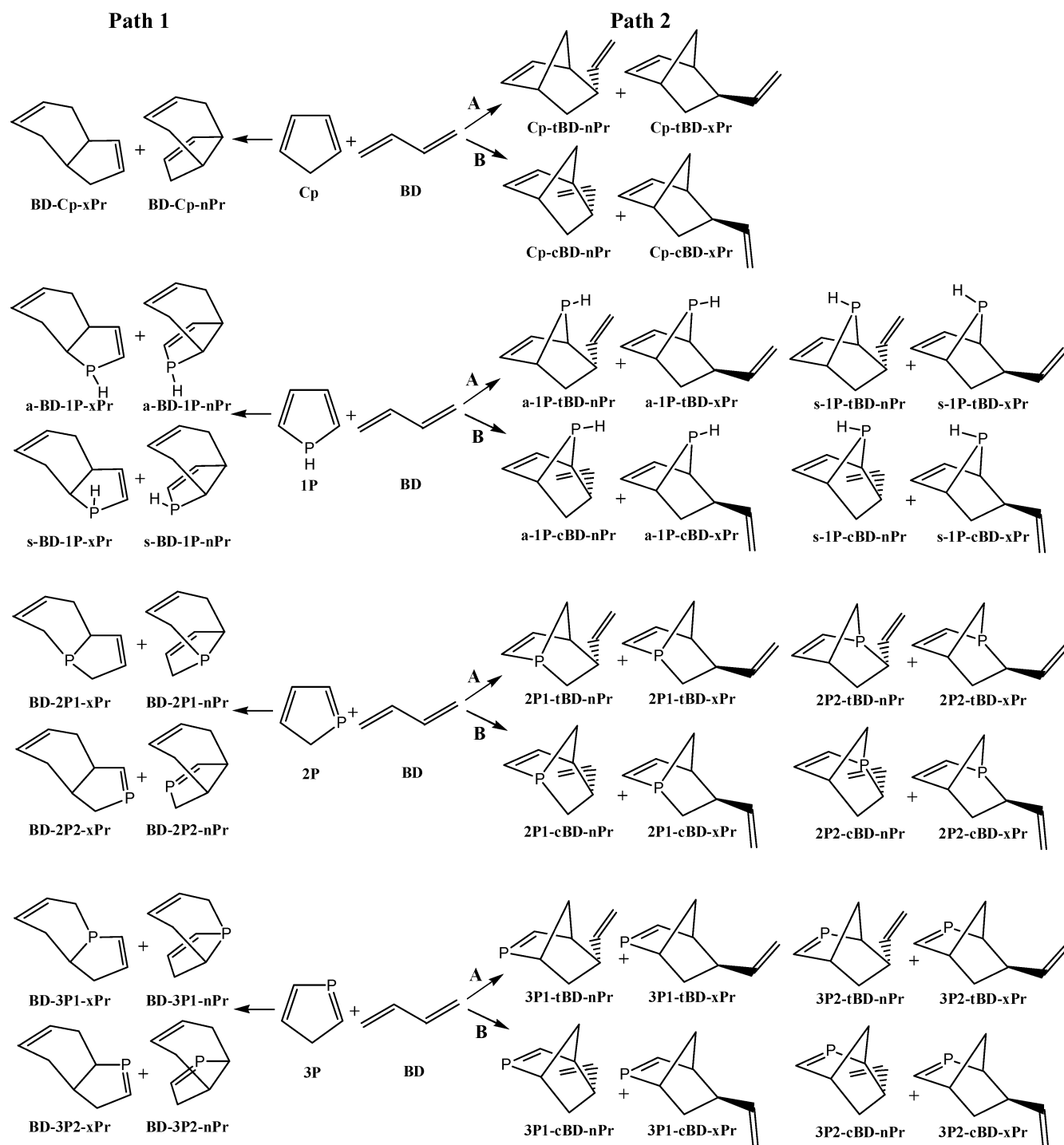
Theoretical studies have well demonstrated that concerted and stepwise mechanisms often compete in thermally allowed cycloadditions.^{25–29} In the Diels–Alder reaction between butadiene and ethylene, the concerted pathway is about 2–8 kcal/mol lower in energy than the lowest energy alternative stepwise path.²⁶ Computational studies on the secondary kinetic isotopic effect on the Diels–Alder reactions support the concerted mechanism and are in agreement with the experimental values.³⁰ There will be competing reaction pathways when both the reactants can serve as the diene and dienophile in the Diels–Alder cycloaddition. Theoretical studies in the direction of exploring these types of competitive reaction pathways are limited so far. The present study addresses the competing reactivities of the reactants by considering the reactions of phospholes with butadiene.

* Corresponding authors. J.L.: e-mail, jerzy@ccmsi.us; tel, 601-979-3482; fax, 601-979-7823. G.N.S.: e-mail, gnsastry@iict.res.in; tel, +91-40-27160123 ext. 2619; fax, +91-40-27160512.

[†] Jackson State University.

[‡] Indian Institute of Chemical Technology.

SCHEME 1



A total of 42 [4+2] cycloaddition possibilities for the reactions of cyclopentadiene, 1*H*-, 2*H*- and 3*H*-phospholes with butadiene are explored using DFT and CCSD(T) methods. The reactions considered may be divided into two categories depending on whether the five-membered ring acts as a diene or dienophile with butadiene. These two categories are shown as pathways 1 and 2 in Scheme 1. A and B in path 2 correspond to reactions involving *s*-*trans* and *s*-*cis* conformers of butadiene as the dienophile.

We address the following questions in the present study: (a) Do phospholes and cyclopentadiene prefer to be the diene or dienophile on reaction with butadiene under thermal conditions? (b) How do the activation and reaction energies vary as the diene–dienophile combinations alter? (c) How effective is the

secondary orbital interaction along the endo-pathway? (d) How many of the endo-TSs are bispericyclic? (e) When butadiene acts as a dienophile, is there any *cis*/*trans*-selectivity? If so, to what extent? (f) How competitive are the intermolecular Diels–Alder reactions compared to the cyclodimerizations? Systematic quantum chemical calculations were carried out to address the above questions.

Computational Details

All the reactants, transition states and products were fully optimized using hybrid density functional theory, the B3LYP level with the 6-31G(d) basis set. Vibrational frequency calculations indicate that transition states obtained possess one

imaginary frequency whose normal mode corresponds to the [4+2] cycloaddition and the products have all real frequencies. Geometry optimizations and frequency calculations were also repeated at the B3LYP/6-311+G(d,p) level and essentially the same conclusions were obtained. Considering the inability to use a high basis set at the CCSD(T) level and the demonstrated excellent performance of the 6-31G(d) basis set in conjunction with the B3LYP level,^{19,29} we have chosen to perform CCSD(T)/6-31G(d) calculations on the B3LYP/6-31G(d) optimized geometries. IRC calculations (with the default mass weighted Cartesian coordinates) were carried out for all the transition states at the B3LYP/6-31G(d) level. IRC calculations are warranted especially for the bispericyclic transition structures, as examination of the transition vector does not lead to unambiguous characterization of the transition structure. All the calculations were performed using the Gaussian 03 program package.³¹

Results and Discussion

Throughout the paper, **BD**, **Cp**, **1P**, **2P** and **3P** represent butadiene, cyclopentadiene, 1*H*-phosphole, 2*H*-phosphole and 3*H*-phosphole, respectively. The letters “n” and “x” are used to denote endo and exo orientations, respectively. Transition states and products are labeled with TS and Pr. The prefixes “a” and “s” for transition states and products in the case of **1P** system indicate the orientation of the P–H bond away (anti) from the diene (**BD**) side and toward (syn) the diene, respectively. For example, **Cp-tBD-xTS** means the exo transition state (**xTS**) formed by addition of **Cp** as the diene with *s-trans*-butadiene (**tBD**) as the dienophile. **2P1**, **2P2**, **3P1** and **3P2** are used for indicating the regioisomeric transition states and products of the reactions involving 2*H*- and 3*H*-phospholes (Figures 1 and 2).

Equilibrium Geometries. The transition state structures with the principal geometric parameters obtained at the B3LYP level using 6-31G(d) and 6-311+G(d,p) basis sets are depicted in Figure 1 and the product geometries in Figure 2. A critical examination of the geometries shown in Figures 1 and 2 points out that the deviation of the bond lengths between 6-31G(d) and 6-311+G(d,p) basis sets is not significant (less than 0.01 Å) except for the forming bond lengths in the transition states. The significant variation in the bond lengths between the two forming bonds indicates that all the transition state structures are asynchronous. Comparison of the geometries obtained at the B3LYP/6-31G(d) with previously reported HF/6-31G(d) geometries for the transition states and products of the reactions of **Cp** and **2P** with **BD** reveal that variations between the two methods are substantial. Considering the excellent performance of B3LYP/6-31G(d) method for modeling the structure and reactivity of this class of compounds, further single point calculations at the CCSD(T) level were done on these geometries. Therefore, we confine our discussion only to the B3LYP/6-31G(d) geometries throughout this paper, unless otherwise specified.

Let us start with the prototype hydrocarbon reaction between **Cp** and **BD**; one out of six transition state structures could not be located. The structure **BD-Cp-nTS** collapsed to **Cp-cBD-nTS** at the B3LYP level, and all our efforts in locating the correct transition state structure were futile. However, both these transition state structures were located at the semiempirical (AM1) and HF/3-21G levels. It should be noted that the transition state **Cp-cBD-nTS** obtained at the B3LYP level appears to possess bispericyclic nature where the transition state has a mix of [4+2] and [2+4] characters. The difference in

bond lengths between the two forming σ -bonds (about 0.6 Å) in **BD-Cp-xTS** indicates the high asynchronous nature of the transition state. In general, the geometries of the four isomeric transition states resulting from addition of **Cp** (diene) with **BD** (dienophile) are very similar except for the different orientation of vinyl group. The asynchronicity is slightly higher in *s-cis*-**BD** involved as the dienophile (0.5–0.7 Å) compared to *s-trans*-**BD** (0.4 Å). Although the previous theoretical study of Bachrach et al. at the HF/6-31G(d) level pointed out the asynchronicity of these transition state structures,²³ the present study indicates that asynchronicity is much higher at the B3LYP level. Earlier computational study reported four products for the addition of **BD** (diene) with **Cp** (dienophile), including the endo (**BD-Cp-nPr**) and exo (**BD-Cp-xPr**) shown in Figure 2. The two products obtained here have a boat conformation for the six-membered ring and near eclipsed orientation across the fused bond whereas the additional two products reported earlier are the six-membered ring in the chair conformation with a staggered form across the fused bond. The present study considered only the products corresponding to the exo and endo transition states, and we are not interested in other possible products.

IRC calculations have unambiguously characterized the transition states in all cases except for **3P1-cBD-nTS**, **a-1P-cBD-nTS** and **s-1P-cBD-nTS**. Surprisingly, in the above three cases, IRC calculations connect each of the transition states to the two cycloaddition products not to the separated reactants. The transition state **3P1-cBD-nTS** is connected to **3P1-cBD-nPr** and **BD-3P1-nPr**, the other two transition states **a-1P-cBD-nTS** and **s-1P-cBD-nTS** connect to the corresponding products and also connect to **s-BD-1P-nPr** and **a-BD-1P-nPr**, respectively, instead of the reactants. However, the IRC calculations on the transition state structure **Cp-cBD-nTS**, which was designated as the bispericyclic transition structure, reveal that it is properly connected to the corresponding reactant and product. The seemingly strange behavior of three bispericyclic TS structures **3P1-cBD-nTS**, **a-1P-cBD-nTS** and **s-1P-cBD-nTS** warranted a closer look at the potential energy surfaces. We have carefully analyzed the potential energy surface, whether it is possible to have alternative TS structures that can properly connect to the reactant and product, but without success. Furthermore, futile attempts were also made to locate any intermediate, other than the two products and the reactant in the vicinity along the path. Thus, the located transition structures appear to be the only stationary points along the trajectory of approach.

The reaction of **BD** with **1P** results in a total of 12 transition states proceeding via path 1 and path 2 (A and B). Four transition states were located with **BD** (diene), where a couple of pathways are possible depending on the disposition of P–H bond orientation with respect to the diene moiety (Figure 1). Considering the orientational variation of the P–H bond, in the reaction between **1P** as the diene and **BD** as the dienophile (path 2), in principle, eight distinct products are possible. All eight corresponding transition structures were located and characterized on the potential energy surface. Six out of eight transition states are normal [4+2] cycloaddition, and two of the structures (**a-1P-cBD-nTS** and **s-1P-cBD-nTS**) are akin to the bispericyclic transition state, exploiting the favorable endo orientation. As mentioned earlier, the distinction of diene and dienophile vanishes in the bispericyclic transition states. Thus, the transition states **a-1P-cBD-nTS** and **s-BD-1P-nTS** are identical, but both of them are depicted in different orientations in Figure 1 for consistency. It should be noted that the normal [4+2] cycloadd-

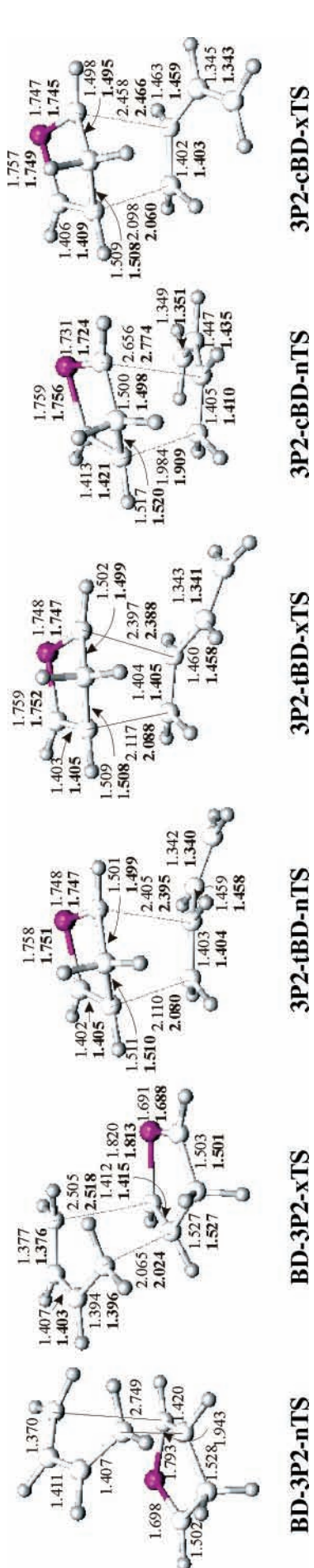


Figure 1. Principal geometric parameters obtained at the B3LYP level with 6-31G(d) (plain) and 6-311+G(d,p) (bold) basis sets for the transition state structures. All the distances are in Å. Structures **BD-Cp-nTS** and **BD-2P2-nTS** were obtained at the AM1 level.

dition transition state **a-BD-1P-nTS** corresponding to product **a-BD-1P-nPr** was located and characterized.

The bond lengths of the transition states **a-1P-tBD-nTS**, **a-1P-tBD-xTS** and **a-1P-cBD-xTS** are very similar, and insignificant deviation in bond lengths is observed among the three transition states **s-1P-tBD-nTS**, **s-1P-tBD-xTS** and **s-1P-cBD-xTS**. The forming bond lengths, near the vinyl group, for the third transition states are about 0.05–0.15 Å longer compared to the other two transition states in the above-mentioned sets. Owing to the strong secondary orbital influence on the transition states **a-1P-cBD-nTS** and **s-1P-cBD-nTS**, the geometries are significantly varied compared to the other three transition states in their respective sets. Like the reactions involving **Cp**, considerable deviation between the forming bond lengths (about 0.5–0.6 Å) is noted in the transition states of the cycloaddition of **1P** with **BD** as the dienophile, indicating high asynchronous character of the reaction pathways. In all the products, the length of the newly formed C–C σ -bond to the carbon bearing the vinyl group is slightly longer than the typical C–C bond length. Furthermore, the C–C single bond resulting from the dienophile C=C in the products via path 1 and path 2A is slightly longer than the normal bond distance. This may be traced to the strain of the ring system.

Similar to **1P** with **BD**, **2P** with **BD** results in a total of 12 cycloaddition products, involving path 1 and 2 (A and B). There are two possibilities of [4+2] cycloaddition of **BD** as the diene with **2P** as the dienophile (path 1); one is addition across C=P and another across C=C. In these cases, four products were obtained but only three transition states could be located at the B3LYP level. The endo transition state for the addition across C=C (**BD-2P2-nTS**) could not be located at the B3LYP level and all the putative structures collapsed to **2P2-cBD-nTS**. The collapsing of the transition state **BD-2P2-nTS** may be ascribed to the beneficial endo orientation and the low barrier required for **2P2-cBD-nTS** due to the conversion of weak C=P to C–P. Previous computational study has reported the transition state **BD-2P2-nTS** at the HF/6-31G(d) level but one of the C \cdots C bonds between the two fragments is almost formed (1.582 Å).²³ Transition state geometries suggest that the asymmetry of the transition state **BD-2P2-xTS** is higher compared to the other two transition states obtained through path 1.

The addition of **2P** (diene) with **BD** (dienophile) can proceed through eight regioisomeric transition states (path 2). All eight transition states and the corresponding products were obtained. The nomenclature starting with **2P1** is given for the structures where the phosphorus atom forms a bond with a terminal carbon (C1) of **BD**, and the structures in which the phosphorus atom makes the bond with carbon (C2 of **BD**) bearing the vinyl group are represented by labels starting with **2P2**. Similar to C–C forming bond lengths in the case of other transition states, the C–P forming bond length near the vinyl group is significantly longer (0.3–0.5 Å) than that of the terminal bond. The transition states (starting with **2P2**) wherein the phosphorus atom forms a bond with the carbon possessing a vinyl group are more asynchronous and looser compared to other regioisomeric transition states (**2P1**). The exo and endo transition state geometries are very similar in the case of addition of **2P** to *s-trans*-**BD** (path 2A) whereas a difference (0.03–0.1 Å) is observed particularly in the forming bond lengths when addition takes place with *s-cis*-**BD** as the dienophile. This geometric discrepancy may be due to either the steric repulsion between the vinyl group of the dienophile fragment and **2P** or the strong secondary orbital influence in the endo transition states. Most of the bond lengths in the product geometries obtained from

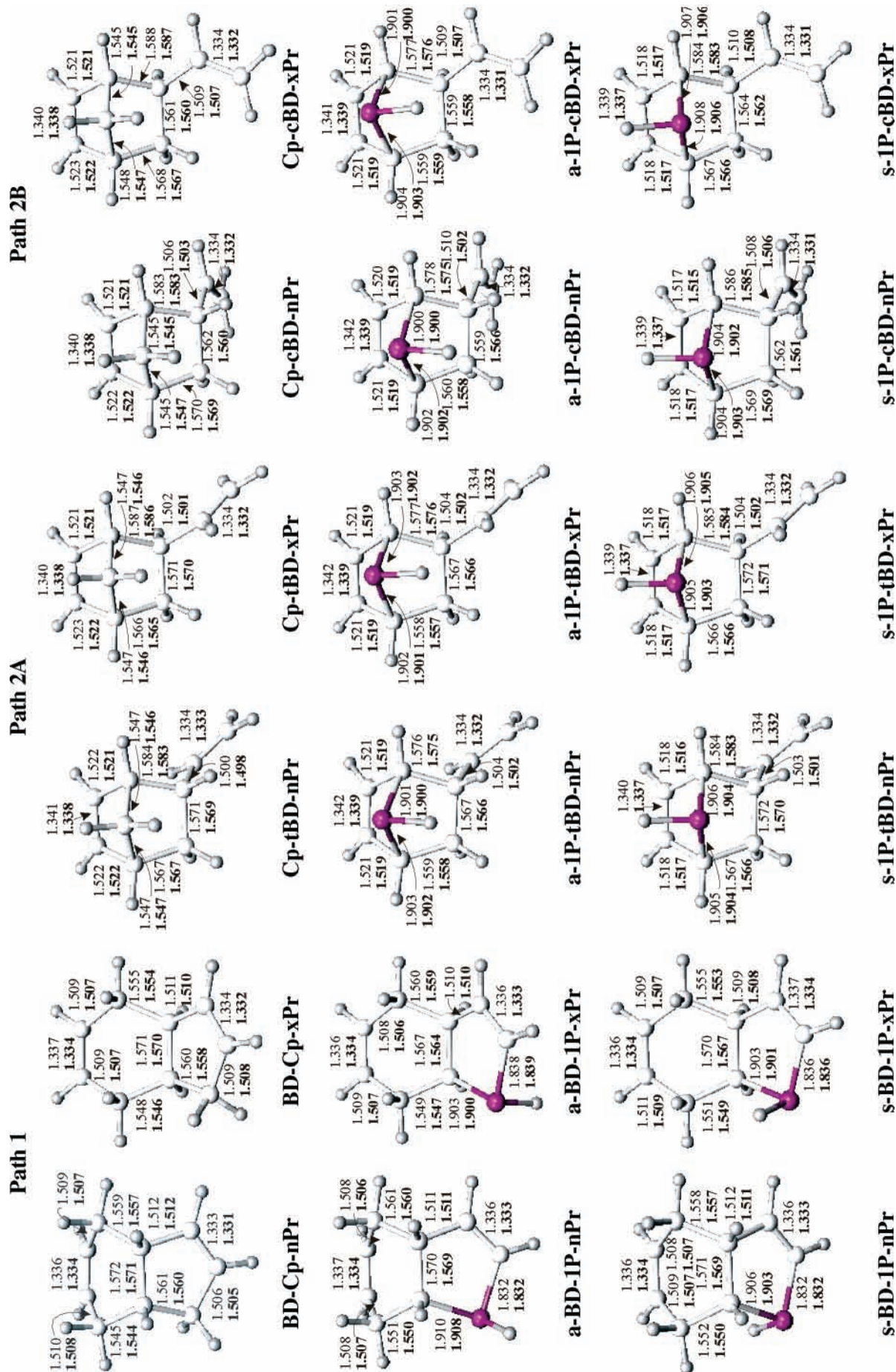


Figure 2. Continued

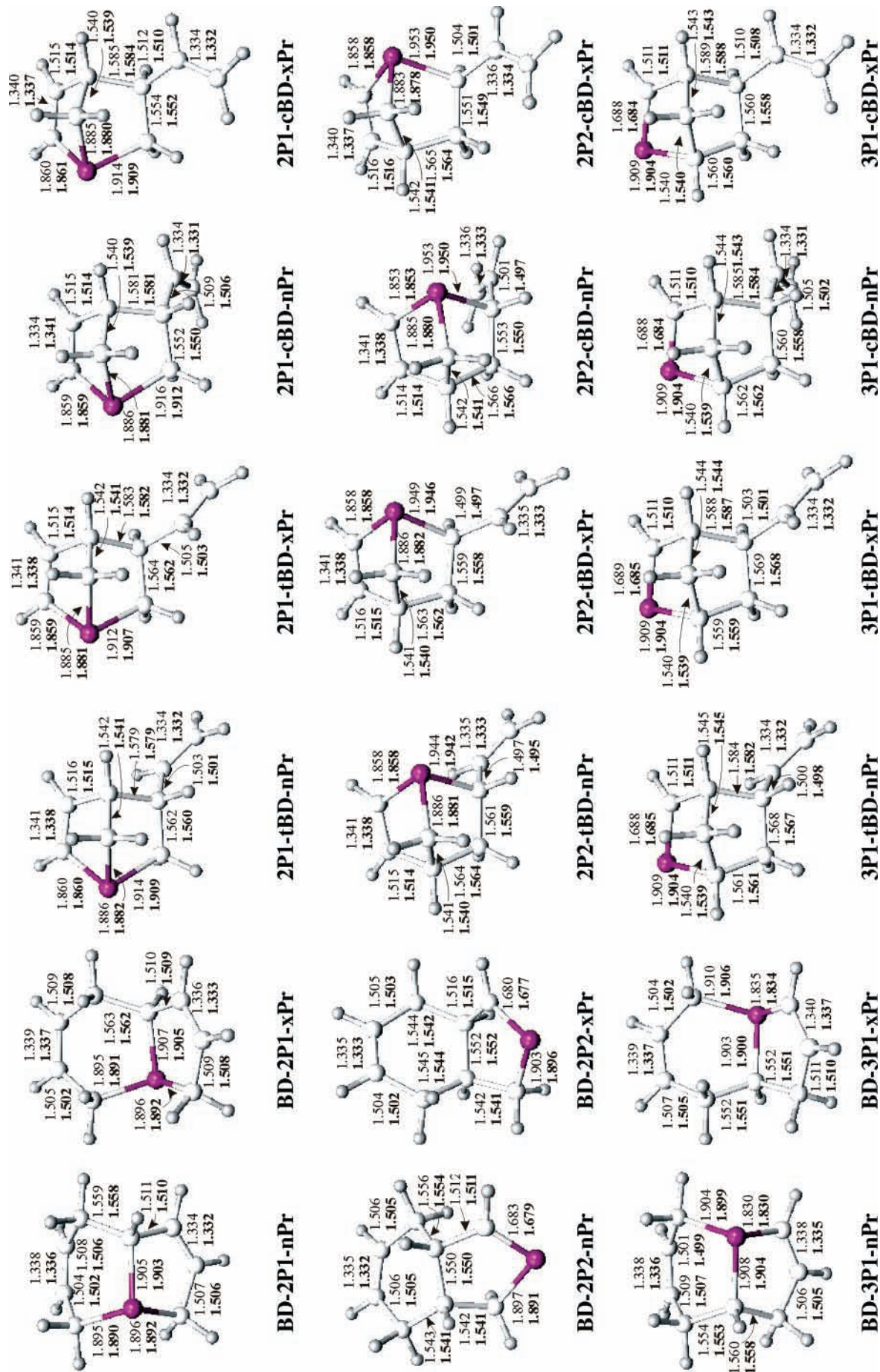


Figure 2. Continued

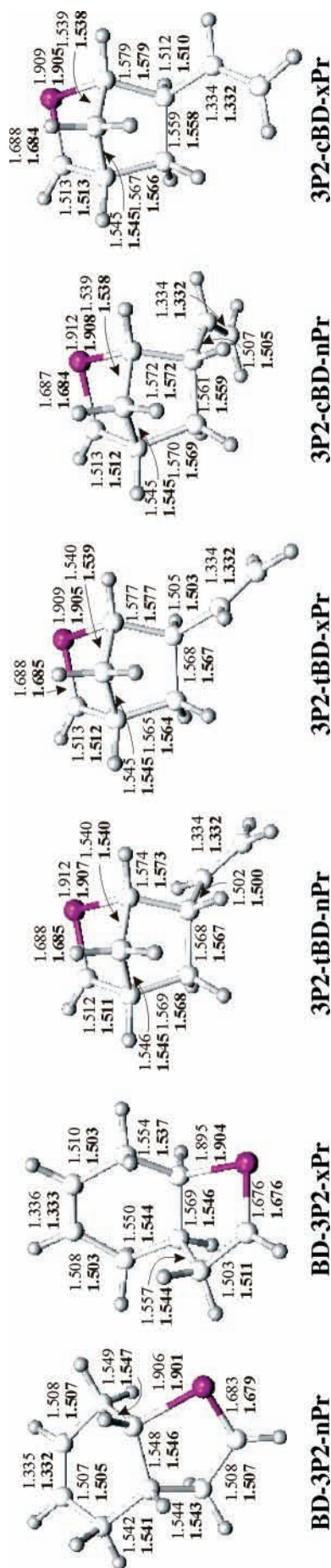


Figure 2. Principal geometric parameters obtained at the B3LYP level with 6-31G(d) (plain) and 6-311+G(d,p) (bold) basis sets for the products of the Diels–Alder cycloadducts. All the distances are in Å.

the reactions involving **2P** are within the expected values but the newly formed C–C or C–P single bonds, which are near to the vinyl group, are longer compared to the normal single bond distances.

Like the reactions involving **2P**, regioisomeric transition states and products are possible in the cycloaddition of **3P** with **BD**. Four transition states and their corresponding products were obtained for the [4+2] addition of **BD** (diene) with **3P** (dienophile); two transition states result from addition of **BD** across C=P and the remaining two through addition across C=C of **3P**. Eight transition states and the corresponding products were obtained in path 2. The structure **BD-3P2-nTS** could be located at the B3LYP/6-31G(d) level but collapsed to **3P2-cBD-nTS** at the B3LYP/6-311+G(d,p) level and all our attempts in locating the transition state structure at this level were futile. The transition state bond lengths show that these four transition states are asynchronous. The difference between the forming bond lengths is much higher for the transition states that result from the addition across C=C of **3P** (dienophile). The geometries of the isomeric transition states **3P1-tBD-nTS**, **3P1-tBD-xTS** and **3P1-cBD-xTS** are very similar whereas **3P1-cBD-nTS** is akin to bispericyclic transition state. One of the C···C bond lengths in **3P1-cBD-nTS** is about 1.58 Å, indicating that the bond is almost formed. Two [4+2] cycloaddition reactions are merged in the bispericyclic transition state **3P1-cBD-nTS**; however, the transition state (**BD-3P1-nTS**) for one of the two [4+2] merged cycloaddition reactions has been successfully located independently. In the reactions of **3P** with **BD** as the dienophile, the transition states (**3P1**) where phosphorus atom is adjacent to the termini of the **BD** are tighter and more asynchronous compared to other regioisomeric transition states (**3P2**) except for **3P2-cBD-nTS**. The bond lengths of **3P2-tBD-nTS** are similar to the corresponding exo transition state. In contrast, the remarkable difference in the forming bond lengths is observed between **3P2-cBD-nTS** and **3P2-cBD-xTS**, this may be attributed to the partially bispericyclic nature or the steric repulsion in the endo transition state (**3P2-cBD-nTS**). In the products of **3P** addition with **BD** (dienophile), many of the newly formed C–C bond distances and the length of the C–C bond converted from the dienophilic C=C bond are longer than the typical C–C bond lengths.

Activation and Reaction Energies. The activation energies calculated at the B3LYP and CCSD(T) levels are given in Table 1, and the reaction energies are listed in Table 2. Figure 3 depicts the energy profile at the CCSD(T)/6-31G(d) level for the reactions considered in Scheme 1. Table 1 shows that B3LYP/6-311+G(d,p) level overestimates the activation energies compared to CCSD(T)/6-31G(d). However, the values obtained at the B3LYP/6-31G(d) level are similar or slightly overestimated compared to the CCSD(T) results. Certain transition states are bispericyclic in nature, where the CCSD(T) level shows a low barrier by about 4–5 kcal/mol. A perusal at Table 1 indicates that many of the activation energies are between 12 and 16 kcal/mol in the case of reactions of **2P** with butadiene. The very low barrier (about 2 kcal/mol) is observed for the addition of **3P** with **BD**, and also the low activation barrier by about 12–15 kcal/mol is predicted for the addition of **BD** across C=P of **3P**. The low activation energies observed in these cases can be attributed to the conversion of weak C=P to C–P from reactants to the products.

Table 2 shows that B3LYP method underestimates the reaction exothermicities compared to the CCSD(T) level. The activation and reaction energies reported at the MP4SDQ/6-31G(d)//HF/6-31G(d) for the reactions of **Cp** and **2P** with **BD**

TABLE 1: Activation Energies (ΔE^\ddagger , kcal/mol) Obtained at the B3LYP/6-31G(d) (I), B3LYP/6-311+G(d,p) (II) and CCSD(T)/6-31G(d) (III) Levels for the Reaction Pathways Considered in Scheme 1 (Structures and Nomenclature in Figure 1)^a

TS str	path 1			path 2								
	I	II	III	A			B					
				TS str	I	II	III	TS str	I	II	III	
BD-Cp-nTS	<i>b</i>	<i>b</i>		Cp-tBD-nTS	22.1	25.3	20.4	Cp-cBD-nTS	22.1	24.7	20.5	
BD-Cp-xTS	23.9	26.8	24.0	Cp-tBD-xTS	21.9	25.2	20.4	Cp-cBD-xTS	23.0	26.2	21.4	
a-BD-1P-nTS	25.5	28.2	23.7	a-1P-tBD-nTS	26.6	29.2	24.3	a-1P-cBD-nTS	24.3	27.2	19.3	
a-BD-1P-xTS	26.4	29.2	25.6	a-1P-tBD-xTS	26.8	29.6	24.7	a-1P-cBD-xTS	27.3	29.9	25.5	
s-BD-1P-nTS	24.3	27.2	19.3	s-1P-tBD-nTS	27.0	29.8	24.2	s-1P-cBD-nTS	23.9	27.1	18.2	
s-BD-1P-xTS	24.3	27.1	24.0	s-1P-tBD-xTS	27.0	30.0	24.5	s-1P-cBD-xTS	29.6	32.4	26.8	
BD-2P1-nTS	12.4	14.0	12.6	2P1-tBD-nTS	12.9	14.9	11.9	2P1-cBD-nTS	12.9	14.5	11.9	
BD-2P1-xTS	15.0	16.7	16.3	2P1-tBD-xTS	12.6	14.8	11.8	2P1-cBD-xTS	13.5	15.6	12.8	
BD-2P2-nTS	<i>c</i>	<i>c</i>		2P2-tBD-nTS	14.4	16.5	12.8	2P2-cBD-nTS	14.9	16.9	13.2	
BD-2P2-xTS	21.6	24.5	21.7	2P2-tBD-xTS	14.5	16.8	12.9	2P2-cBD-xTS	14.9	17.4	13.2	
BD-3P1-nTS	13.0	15.1	12.6	3P1-tBD-nTS	20.3	23.4	19.3	3P1-cBD-nTS	6.8	11.8	2.2	
BD-3P1-xTS	14.2	16.4	14.7	3P1-tBD-xTS	20.2	23.4	19.3	3P1-cBD-xTS	21.4	24.4	20.3	
BD-3P2-nTS	25.2	<i>d</i>	23.3	3P2-tBD-nTS	24.2	27.3	21.9	3P2-cBD-nTS	25.0	27.5	22.5	
BD-3P2-xTS	25.7	28.4	25.0	3P2-tBD-xTS	23.8	26.9	21.6	3P2-cBD-xTS	24.8	27.8	22.4	

^a Single point calculations were done at the CCSD(T) level on the B3LYP/6-31G(d) geometries. ^b Collapsed to **Cp-cBD-nTS**. ^c Collapsed to **2P2-cBD-nTS**. ^d Collapsed to **3P2-cBD-nTS**.

TABLE 2: Reaction Energies (ΔE_r , kcal/mol) Obtained at the B3LYP/6-31G(d) (I), B3LYP/6-311+G(d,p) (II) and CCSD(T)/6-31G(d) (III) Levels for the Reaction Pathways Considered in Scheme 1 (Structures and Nomenclature in Figure 2)^a

PR str	path 1			path 2								
	I	II	III	A			B					
				PR str	I	II	III	PR str	I	II	III	
BD-Cp-nPr	-30.6	-24.0	-38.8	Cp-tBD-nPr	-16.5	-10.3	-26.6	Cp-cBD-nPr	-14.8	-8.7	-25.2	
BD-Cp-xPr	-30.9	-24.5	-38.7	Cp-tBD-xPr	-16.2	-10.2	-26.3	Cp-cBD-xPr	-14.9	-8.8	-25.2	
a-BD-1P-nPr	-26.2	-20.0	-35.1	a-1P-tBD-nPr	-13.3	-7.9	-24.1	a-1P-cBD-nPr	-11.3	-6.0	-24.1	
a-BD-1P-xPr	-27.0	-21.1	-35.5	a-1P-tBD-xPr	-12.9	-7.5	-23.6	a-1P-cBD-xPr	-11.5	-6.1	-22.3	
s-BD-1P-nPr	-26.3	-20.2	-35.1	s-1P-tBD-nPr	-11.1	-5.9	-22.2	s-1P-cBD-nPr	-9.3	-4.2	-20.6	
s-BD-1P-xPr	-27.1	-21.0	-35.4	s-1P-tBD-xPr	-10.8	-5.7	-21.8	s-1P-cBD-xPr	-9.0	-3.7	-20.1	
BD-2P1-nPr	-28.0	-23.6	-34.5	2P1-tBD-nPr	-19.4	-15.1	-28.3	2P1-cBD-nPr	-17.8	-13.6	-26.8	
BD-2P1-xPr	-26.9	-22.6	-33.0	2P1-tBD-xPr	-19.0	-14.9	-27.8	2P1-cBD-xPr	-17.8	-13.6	-26.7	
BD-2P2-nPr	-27.0	-20.9	-36.5	2P2-tBD-nPr	-19.4	-15.3	-28.0	2P2-cBD-nPr	-18.1	-14.1	-27.0	
BD-2P2-xPr	-26.6	-20.6	-36.0	2P2-tBD-xPr	-19.1	-15.0	-27.7	2P2-cBD-xPr	-18.4	-14.3	-27.0	
BD-3P1-nPr	-31.8	-26.7	-36.9	3P1-tBD-nPr	-18.7	-12.9	-29.0	3P1-cBD-nPr	-17.1	-11.2	-27.7	
BD-3P1-xPr	-31.8	-26.7	-36.7	3P1-tBD-xPr	-18.7	-12.9	-28.9	3P1-cBD-xPr	-17.4	-11.5	-27.8	
BD-3P2-nPr	-30.8	-24.4	-39.2	3P2-tBD-nPr	-18.1	-12.2	-28.5	3P2-cBD-nPr	-17.0	-10.9	-27.7	
BD-3P2-xPr	-28.0	-24.5	-35.8	3P2-tBD-xPr	-18.6	-12.9	-29.1	3P2-cBD-xPr	-17.3	-11.5	-27.9	

^a Single point calculations were done at the CCSD(T) level on the B3LYP/6-31G(d) geometries.

by Bachrach and Perriott are compared with the present results.²³ The activation energies reported in the earlier study are higher than the values obtained at any of the levels in the current study and were overestimated by about 5–8 kcal/mol compared to the CCSD(T) level. The reaction exothermicities reported at the MP4SDQ level were slightly underestimated compared to the CCSD(T), albeit the trends obtained are similar.²³ In this section, only CCSD(T) results are employed for discussion unless otherwise specified.

A quick look at Figure 3 shows that the lowest activation barrier for the reactions involving cyclopentadiene (**Cp**) and 1*H*-phosphole (**1P**) with butadiene (**BD**) is about 20 and 18 kcal/mol whereas the value is about 12 kcal/mol in the case of 2*H*-phospholes. It should be noted that the lowest barrier for 3*H*-phosphole is about 2 kcal/mol. The highest exothermicity values are born by **3P** with butadiene, in the range -27 to -40 kcal/mol. However, comparing the reactivities of all five-membered rings, the reactions of **2P** with butadiene are expected to be highly viable kinetically. Considering the reactivity of individual sets, most of the reactions are highly competitive among path 1, path 2A and path 2B. The reaction between **Cp** and **BD** shows that path 2A, where the former acts as the diene, is about 4.0 kcal/mol kinetically more favored than path 1 and 0.1–1.0 kcal/mol more favored than path 2B. In the case of the reaction

between **1P** and **BD**, the transition states in both paths (1 and 2) lie between 18 and 27 kcal/mol with respect to the reactants energy. Path 2B is highly favored via endo orientation for both syn and anti. The difference in energy between the endo and the corresponding exo transition state is much less with *trans*-**BD** as the dienophile. However, the endo preference of *cis*-**BD** for the transition state is prominent, obviously due to the favorable secondary orbital interactions. Table 2 shows that exo products are slightly more stable than that of the endo in the case of **1P** as the dienophile with **BD**.

Table 1 and Figure 3 clearly show that, in agreement with the previous computational study,²³ the reaction of **2P** with **BD** is very similar to the hydrocarbon system, i.e., the reaction between **Cp** and **BD**. However, the activation energies required for the former reaction are significantly lower than the latter. **2P** with **BD** bears activation energies of 11–22 kcal/mol and is highly competitive where path 2A is more preferred compared to path 1 and path 2B. Table 2 indicates that the exothermicities for the reaction of **2P** with **BD** through paths 2A and 2B are increased by about 1–2 kcal/mol whereas they are decreased by about 2–6 kcal/mol for the reaction proceeding via path 1 compared to the hydrocarbon case. The transition states of the reactions of **2P** as the diene and **BD** as the dienophile (path 2) are about 12–13 kcal/mol above to the reactants energy whereas

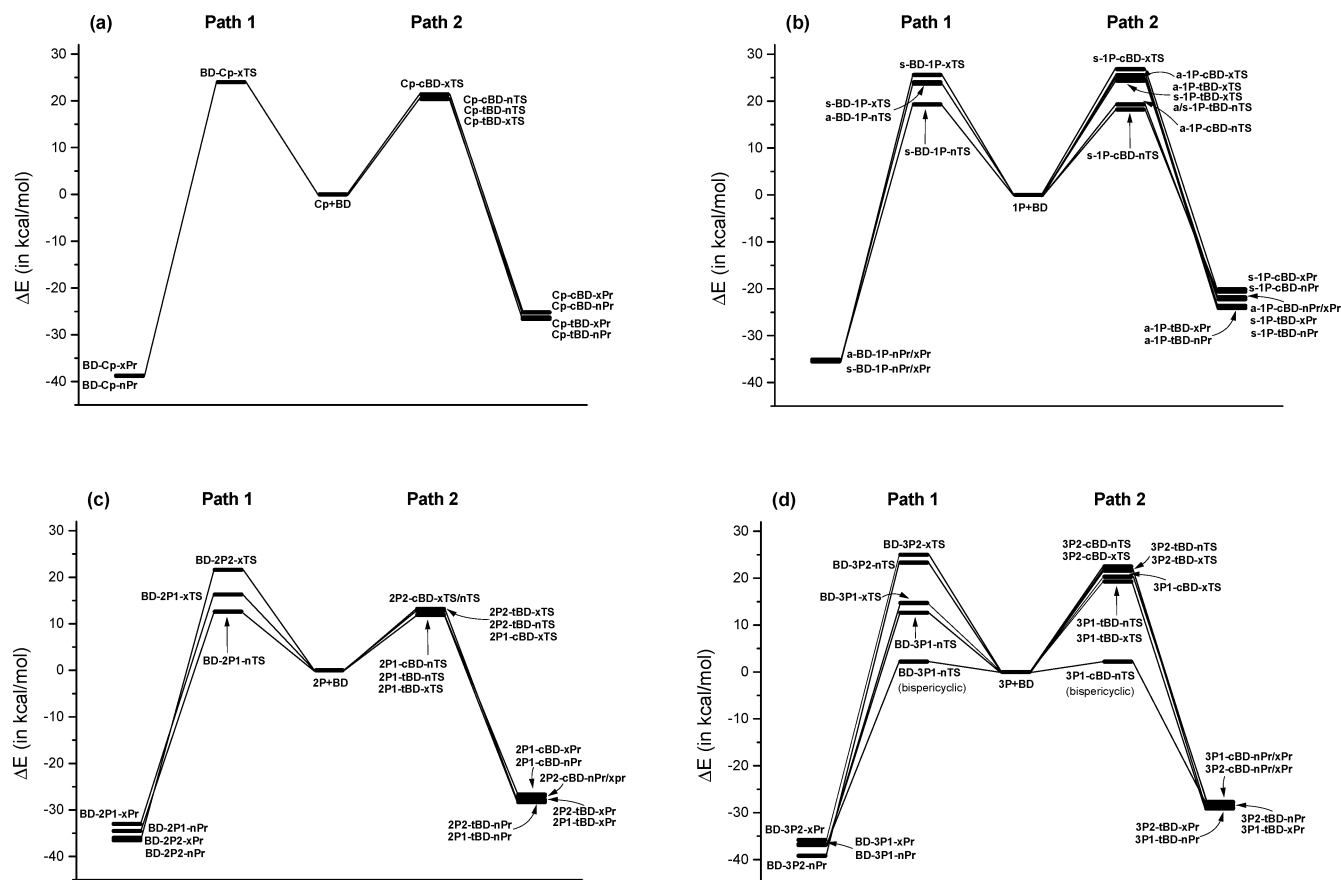


Figure 3. Energy profile for the diene–dienophile competitive Diels–Alder reaction pathways of cyclopentadiene and phospholes with butadiene. Relative energies are given at the CCSD(T)/6-31G(d) level.

the activation barriers are between 12 and 22 kcal/mol along path 1 where **BD** is the diene. This barrier is similar to or slightly less than that required in the case of reactions of **Cp** and **1P** with **BD**. The cycloaddition of **BD** as the diene across the C=P of **2P** through endo attack (**BD-2P1-nTS**) requires the activation energy of 12.6 kcal/mol that is the lowest barrier in path 1. This transition state lies only 0.8 kcal/mol above and 0.6 kcal/mol below, corresponding to the lowest and the highest energy transition state structures in path 2. Thus, our results demonstrate that there can be competition between pathways 1 and 2. However, the reaction of **BD** as the diene to the addition across C=P of **2P** (path 1) is predicted to be highly favored, which is in agreement with the previous computational study of Bachrach and Perriott,²³ and the results confirm the experimental observation of Mathey that the major product is the addition of **BD** across C=P of **2P**. Mathey also reported another unidentified minor product in the reaction of *2H*-phosphole with **BD**.^{13b} Table 2 indicates that the endo product from the addition of **BD** across C=P of **2P** (**BD-2P1-nPr**) is more stable by about 1 kcal/mol than the product obtained by addition across C=C of **2P** (**BD-2P2-nPr**) at the B3LYP/6-31G(d) level; this result supports Mathey's experimental observation of the former product reported as major.^{13b} However, the product stability order is predicted opposite at the CCSD(T) level with the energy difference of 2 kcal/mol.

In the case of **3P** with **BD**, activation barriers range from 2 to 25 kcal/mol, where the value 2.2 kcal/mol is born by **3P1-cBD-nTS** that is a bispericyclic transition state. Except for this, path 1 is kinetically more favored for the **3P1** regioisomer and path 2A is more preferred for the **3P2** regioisomer. In contrast to other cases, a very low barrier (about 2 kcal/mol) is observed for the reaction of **3P** with **BD** through the bispericyclic

transition state (**3P1-cBD-nTS**), which seems to be common to both **3P1-cBD-nPr** and **BD-3P1-nPr**. The product **BD-3P1-nPr** is more stable by about 9 kcal/mol than **3P1-cBD-nPr**. Although the transition state **3P1-cBD-nTS** is the combination of two cycloaddition reactions, namely, **3P** (diene) with *cis*-**BD** (dienophile) and *cis*-**BD** addition across C=P of **3P** through endo orientation, the normal [4+2] cycloaddition transition state (**BD-3P1-nTS**) for the latter reaction was located that is 12.6 kcal/mol above the reactants. The low barrier observed may be attributed to the conversion of weak C=P to C–P from reactant to the product. The reaction through pathway 1, addition across C=P of **3P**, in the case of **BD** with **3P** is predicted to be kinetically as well as thermodynamically controlled. The low activation energy and high exothermicity indicate that the reaction of **3P** with butadiene is highly viable. The activation barriers required for the addition of **3P** as the diene with **BD** as the dienophile range from 19 to 22.5 kcal/mol excluding the bispericyclic transition state.

Figure 3 and Table 1 clearly indicate that in the cases of both *2H*- and *3H*-phospholes, in general, the activation barriers are about 7–11 kcal/mol less for the reactions where the conversion of C=P to C–P occurs from reactant to product. This is in harmony with the previous computational studies of Diels–Alder reactions of **2P** and **3P** with different dienophiles and cyclodimerization reactions of these phospholes.^{16,17} However, the results are different when the reaction energies are considered. The products obtained through path 1, where butadiene and the five-membered ring are the diene and dienophile, respectively, are more stable than the corresponding products via path 2 in all the reactions considered. This can be attributed to the lower strain in the bicyclo[4.3.0]nonadiene skeleton compared to the norbornene framework, which results from path

2. Reactions of **1P** with **BD** are the least exothermic in the case of phospholes and also less exothermic compared to the reactions of **Cp** with **BD**. The reactions of **3P** are slightly more exothermic compared to **2P**. The high barrier and the least exothermicity for the reactions of **1P** may be attributed to the slight aromatic character of 1*H*-phosphole (**1P**). Exo vs endo selectivity of the transition states and products, and cis vs trans selectivity of butadiene in the reactions considered are discussed in the forthcoming paragraphs.

In the reactions of **BD** as the diene and cyclic five-membered rings as the dienophiles, the endo transition states are expected to be lower in energy than the corresponding exo, owing to the favorable secondary orbital interaction in the former mode. Table 1 shows that it is intricate to predict the exo–endo selectivity in most cases of the reactions of **2P** and **3P** with *cis*- and *trans*-**BD** as the dienophile fragment because the activation energy differences between the exo and the endo transition states are negligible. It should be noted that the bispericyclic transition state **3P1-cBD-nTS** is remarkably more stable than the corresponding exo transition state.

In contrast to **1P** and analogous to **Cp**, the endo products are more stable than the corresponding exo in the case of **2P** and **3P** participating as dienophiles. Our results indicate that in the reactions of **Cp**, **1P** and **2P** with **BD** as the dienophile, in general, endo products are slightly more stable than the corresponding exo, and it is not very clear in the case of **2P** addition with *cis*-**BD**. In contrast, the exo products are slightly more favored than that of endo in **3P** reaction with **BD** as the dienophile with an exception noticed for **3P1-tBD-xPr**, which is almost similar in energy to **3P1-tBD-nPr**. Activation and reaction energy data from Tables 1 and 2 clearly indicate, in general, the trans selectivity of butadiene. The low barriers observed for the reactions proceeding through bispericyclic transition states suggest the preference of cis conformation of **BD** over trans. The lower stability of the products obtained via path 2B, where *cis*-**BD** acts as the dienophile, compared to path 2A may be due to the steric repulsion between the vinyl group and part of norbornene skeleton containing C=C.

For the pathway in which **BD** acts as the dienophile, the phosphorus atom prefers to bond with the terminal carbon rather than the second carbon atom (C2) of **BD** in the case of reaction with **2P**, and the phosphorus atom prefers to locate near the terminal carbon of **BD** in the case of reaction occurring with **3P**. The difference in product stability ordering is noticed between B3LYP and CCSD(T) levels in the reactions of **BD** as the diene with **2P** and **3P** as the dienophiles. The B3LYP method predicts that the products obtained from the cycloaddition of **BD** across C=P are more stable than across C=C of **2P** as well as **3P**, but the situation is reversed at the CCSD(T) level. Results at the B3LYP level support Mathey's experimental observation of the major product resulting via the addition across the C=P of 2*H*-phospholes.^{13b} It is to be noted that reactions of 3*H*-phospholes are more exothermic than reactions involving 1*H*- and 2*H*-phospholes.

The relative stabilities of three phospholes and the barriers for the interconversion through [1,5] sigmatropic shifts are listed in Table 3. **2P** is more stable than **3P** and **1P**. Interestingly, the barriers for the cycloaddition of **3P** with **BD** are lower and the reactions are more exothermic compared to the other two phospholes. Hence, we would like to examine the interconversion barriers among the three phospholes and the synthetic viability of **3P**. Table 3 indicates that the conversion from **2P** to **1P** is about 5 kcal/mol lower than conversion from **2P** to **3P**. Furthermore, the cyclodimerization reactions of **2P** require

TABLE 3: Relative Stabilities of the Three Phospholes and the Activation Barriers for the Interconversion through [1,5] Sigmatropic Shifts Obtained at the B3LYP/6-31G(d) and the CCSD(T)/6-31G(d)//B3LYP/6-31G(d) Levels (Values in kcal/mol)^a

structure	B3LYP/6-31G(d)	CCSD(T)/6-31G(d)//B3LYP/6-31G(d)
1P	0.0	0.0
2P	-4.8	-7.3
3P	-0.3	-4.0
Activation Barriers		
1P to 2P	19.3	21.0
2P to 1P	24.1	28.3
2P to 3P	29.4	32.9
3P to 2P	24.9	29.6
3P to 3P	27.6	32.3

^a The values were taken from ref 16.

TABLE 4: Activation Barriers of the Lowest (Plain) and Highest (Bold) Values and Reaction Energies of the Most (Plain) and Least (Bold) Exothermic Obtained at the B3LYP/6-31G(d) Level for the Reactions of Cyclopentadiene (Cp), Phospholes (1P, 2P and 3P) with Butadiene (BD) Are Given along with the Values for the [4+2] Cyclodimerizations of Each of the Reactants (Values in kcal/mol)

reaction	path 1		path 2a		path 2b		[4+2] cyclodimerization of five-membered rings ^{a,b}	
	ΔE^\ddagger	ΔE_r	ΔE^\ddagger	ΔE_r	ΔE^\ddagger	ΔE_r	ΔE^\ddagger	ΔE_r
Cp + BD	23.9	-30.9	22.0	-16.5	22.1	-14.9	19.4	-17.4
		-30.6	22.1	-16.2	23.0	-14.8	22.2	-16.3
1P + BD	24.3	-27.1	26.6	-13.3	23.9	-11.5	25.8	-10.6
	26.4	-26.2	27.0	-10.8	29.6	-9.0	29.1	-7.3
2P + BD	12.4	-28.0	12.6	-19.4	12.9	-18.4	2.3	-25.7
	21.6	-26.6	14.5	-19.0	14.9	-17.8	13.7	-13.2
3P + BD	13.0	-31.8	20.2	-18.8	6.8	-17.4	8.5	-24.3
	25.7	-28.0	24.2	-18.1	25.0	-17.0	25.2	-15.7

^a The values are taken from ref 17. ^b The values for **BD** dimerizations are calculated in this work. $\Delta E^\ddagger = 17.7$ (**22.0**) and $\Delta E_r = -39.3$ (**-37.4**).

lower barriers than for the conversion of **2P** to **3P**.¹⁷ Although the possibility of **2P** to **3P** conversion via a [1,5] sigmatropic shift is much lower in unsubstituted systems, suitable substitution may be an effective strategy to obtain **3P** by this route. The **3P** and substituted **3P** thus generated are very much amenable for participation in the cycloaddition reactions.^{16,18}

Comparison with Cyclodimerization. Cyclodimerizations of phospholes through [4+2] addition have been demonstrated as feasible reactions recently.¹⁷ Thus, the possibility of cyclodimerizations of each of the reactants cannot be precluded in the reactions considered. Activation and reaction energies of the lowest and the highest values obtained at the B3LYP/6-31G(d) level for the cycloadditions considered in this study with the values for the cyclodimerizations of each of the reactants are given in Table 4. The comparison of the values exemplifies that the cyclodimerization of **BD** is practical due to the low barrier and high exothermicity. Cyclodimerization of **Cp** is slightly more favored (by about 2.5–4 kcal/mol) kinetically compared to the Diels–Alder reactions with **BD**. In contrast, the reaction between **1P** and **BD** through path 1 is predicted to be more preferred than the cyclodimerization of **1P**. Similar to **Cp**, the cyclodimerizations of **2P** are more favored than the reactions of **2P** with **BD**.

The lowest barrier for the cyclodimerizations of **2P** is about 2 kcal/mol whereas that required for the cycloaddition of **2P** with **BD** is 13 kcal/mol. Thus, the cyclodimerizations of **2P** are highly favored reaction channels in the case of reactions involving **2P**. The present computational study validates the

experimental observation of Mathey that in the reaction of **2P** with various dienophiles, **2P** cyclodimerization takes place initially resulting in a P–P bonded [4+2] dimer, which can then be trapped by various dienophiles.^{12,13} Although pathways 1, 2A and 2B are highly competitive in the case of **2P**, the products through path 1 are computed to be major in yield under thermal conditions that confirm the experimental results of Mathey.^{13b} The reactions via path 1 are highly exothermic in all the cases, indicating that under thermal conditions, the products resulting from path 1 are expected to be major yield. The B3LYP/6-31G(d) level predicts that the cyclodimerization of **3P**, which is **3P** (4π) addition across C=P (2π) of **3P** (see **3P-TS-endo2** and **3P-Pr-endo2**),¹⁷ and the cycloaddition of **3P** with **BD** are in competition; the cycloaddition is slightly more favored than the cyclodimerization. This study predicts that under thermal conditions, as observed in the case of **2P**, the cyclodimers of **3P** formed in the competing reactions may be trapped by **BD**, resulting in the products possessing bicyclo[4.3.0]nonadiene skeleton.

Conclusions

The present study systematically explores the Diels–Alder reactions of phospholes with butadiene considering the reactants as both the diene and dienophile at the B3LYP level using 6-31G(d) and 6-311+G(d,p) basis sets, augmented by the single point CCSD(T)/6-31G(d) calculations. The results are compared with the reaction between cyclopentadiene and butadiene. Transition state geometries reveal that many of the transition states are highly asynchronous although the reactions are concerted. The bispericyclic transition state structures can occur in the reactions where the reactants act as both the diene and dienophile. IRC calculations indicate that three bispericyclic TS structures **3P1-cBD-nTS**, **a-1P-cBD-nTS** and **s-1P-cBD-nTS**, where one of the forming C···C bonds is almost formed, have not connected to the reactants. We have found a similarity in all the systems that the reaction pathway (path 1) wherein butadiene acts as the diene and the cyclic five-membered ring acts as the dienophile is thermodynamically controlled. The high stability of products possessing the bicyclo[4.3.0]nonadiene skeleton, which resulted from path 1, may be attributed to the lower strain, compared to the corresponding norbornene derivatives obtained through path 2. In complete agreement with the experimental report,^{13b} cyclodimerization of **2P** is predicted to be formed initially, resulting in P–P bonded dimer, which can then be trapped by the butadiene. The cyclodimerization of **3P** and the cycloaddition of **3P** with **BD** are predicted to be competitive; the latter reaction is slightly more favored than the former. The present computational study enhances our understanding on the reactivity of phospholes with butadiene and would stimulate experimental interest. Our results predict that Diels–Alder reaction between *3H*-phosphole and butadiene are highly viable; thus the experimental realization of this reaction should be rewarded.

Acknowledgment. This study was supported by NSF EPSCoR Grant No. 99-01-0072-08. T.C.D. and J.L. thank the Mississippi Center for Supercomputing Research (MCSR) for the computational facilities. G.G. thanks CSIR for the Junior Research Fellowship.

Supporting Information Available: Total energies obtained at B3LYP and CCSD(T) levels, thermochemical data at the B3LYP level, B3LYP/6-31G* optimized Cartesian coordinates

for all the reactants, transition states and products. This material is available free of charge via the Internet at <http://pubs.acs.org>.

References and Notes

- (1) Nicolaou, K. C.; Snyder, S. A.; Montagnon, T.; Vassilikogiannakis, G. *Angew. Chem., Int. Ed.* **2002**, *41*, 1668.
- (2) Bird, C. W. In *Comprehensive Heterocyclic Chemistry II*; Katritzky, A. R., Rees, C. W., Scriven, E. F. V., Eds.; John Wiley and Sons: New York, 1996; Vol. 2.
- (3) (a) Carruthers, W. *Cycloaddition Reactions in Organic Synthesis; Tetrahedron Organic Chemistry Series*; Pergamon: Elmsford, NY, 1990. (b) Boger, D. L. *Chem. Rev.* **1986**, *86*, 781.
- (4) Houk, K. N.; Li, Y.; Evanseck, J. D. *Angew. Chem., Int. Ed. Engl.* **1992**, *31*, 682.
- (5) (a) Punnagai, M.; Dinadayalane, T. C.; Sastry, G. N. *J. Phys. Org. Chem.* **2004**, *17*, 152. (b) Dinadayalane, T. C.; Punnagai, M.; Sastry, G. N. *J. Mol. Struct. (THEOCHEM)* **2003**, *626*, 247. (c) Dinadayalane, T. C.; Sastry, G. N. *J. Chem. Soc., Perkin Trans. 2* **2002**, 1902.
- (6) Mathey, F. *Acc. Chem. Res.* **2004**, *37*, 954.
- (7) Mathey, F. *Angew. Chem., Int. Ed.* **2003**, *42*, 1578.
- (8) (a) Mathey, F. *Acc. Chem. Res.* **1992**, *25*, 90. (b) Mathey, F. *Chem. Rev.* **1988**, *88*, 429.
- (9) Deschamps, B.; Ricard, L.; Mathey, F. *Organometallics* **2003**, *22*, 1356.
- (10) Toullec, P.; Ricard, L.; Mathey, F. *J. Org. Chem.* **2003**, *68*, 2803.
- (11) Clochard, M.; Mattmann, E.; Mercier, F.; Ricard, L.; Mathey, F. *Org. Lett.* **2003**, *5*, 3093.
- (12) de Lauzon, G.; Charrier, C.; Bonnard, H.; Mathey, F.; Fischer, J.; Mitschler, A. *J. Chem. Soc., Chem. Commun.* **1982**, 1272.
- (13) (a) Charrier, C.; Bonnard, H.; de Lauzon, G.; Mathey, F. *J. Am. Chem. Soc.* **1983**, *105*, 6871. (b) Mathey, F.; Mercier, F.; Charrier, C.; Fischer, J.; Mitschler, A. *J. Am. Chem. Soc.* **1981**, *103*, 4595. (c) Charrier, C.; Bonnard, H.; Mathey, F. *J. Org. Chem.* **1982**, *47*, 2376.
- (14) (a) Mathey, F.; Mercier, F. *C. R. Acad. Sci. Paris, Ser. IIB* **1997**, *324*, 701. (b) Laporte, F.; Mercier, F.; Ricard, L.; Mathey, F. *Bull. Soc. Chim. Fr.* **1993**, *130*, 843. (c) Le Goff, P.; Mathey, F.; Ricard, L. *J. Org. Chem.* **1989**, *54*, 4754.
- (15) (a) Zhang, Z.; Zhu, G.; Jiang, Q.; Xiao, D.; Zhang, X. *J. Org. Chem.* **1999**, *64*, 1774. (b) Zhang, X.; Jiang, Q.; Xiao, D.; Zhang, Z.; Chao, P. *Angew. Chem. Int. Ed. Engl.* **1999**, *38*, 516. (c) Zhang, X.; Jiang, Q.; Jiang, Y.; Xiao, D.; Chao, P. *Angew. Chem., Int. Ed. Engl.* **1998**, *37*, 1100.
- (16) Dinadayalane, T. C.; Geetha, K.; Sastry, G. N. *J. Phys. Chem. A* **2003**, *107*, 5479.
- (17) Dinadayalane, T. C.; Sastry, G. N. *Organometallics* **2003**, *22*, 5526.
- (18) (a) Geetha, K.; Dinadayalane, T. C.; Sastry, G. N. *J. Phys. Org. Chem.* **2003**, *16*, 298. (b) Geetha, K.; Sastry, G. N. *Indian J. Chem.* **2003**, *42A*, 11.
- (19) (a) Dinadayalane, T. C.; Vijaya, R.; Smitha, A.; Sastry, G. N. *J. Phys. Chem. A* **2002**, *106*, 1627. (b) Vijaya, R.; Dinadayalane, T. C.; Sastry, G. N. *J. Mol. Struct. (THEOCHEM)* **2002**, 589–590, 291.
- (20) Bachrach, S. M.; Perriotti, L. *J. Org. Chem.* **1994**, *59*, 3394.
- (21) (a) Bachrach, S. M. *J. Org. Chem.* **1994**, *59*, 5027. (b) Bachrach, S. M. *J. Org. Chem.* **1993**, *58*, 5414.
- (22) Salzner, U.; Bachrach, S. M. *J. Organomet. Chem.* **1997**, *529*, 15.
- (23) Bachrach, S. M.; Perriotti, L. M. *Can. J. Chem.* **1996**, *74*, 839.
- (24) Mattmann, E.; Simonutti, D.; Ricard, L.; Mercier, F.; Mathey, F. *J. Org. Chem.* **2001**, *66*, 755. (b) Mattmann, E.; Mathey, F.; Sevin, A.; Frison, G. *J. Org. Chem.* **2002**, *67*, 1208.
- (25) Sakai, S. *J. Phys. Chem. A* **2000**, *104*, 922.
- (26) (a) Goldstein, E.; Beno, B.; Houk, K. N. *J. Am. Chem. Soc.* **1996**, *118*, 6036. (b) Beno, B. R.; Wilsey, S.; Houk, K. N. *J. Am. Chem. Soc.* **1999**, *121*, 4816.
- (27) Houk, K. N.; Beno, B. R.; Nendel, M.; Black, K.; Yoo, H. Y.; Wilsey, S.; Lee, J. K. *J. Mol. Struct. (THEOCHEM)* **1997**, *398–399*, 169.
- (28) Leach, A. G.; Goldstein, E.; Houk, K. N. *J. Am. Chem. Soc.* **2003**, *125*, 8330.
- (29) Guner, V.; Khuong, K. S.; Leach, A. G.; Lee, P. S.; Bartberger, M. D.; Houk, K. N. *J. Phys. Chem. A* **2003**, *107*, 11445.
- (30) (a) Singleton, D. A.; Merrigan, S. R.; Liu, J.; Houk, K. N. *J. Am. Chem. Soc.* **1997**, *119*, 3385. (b) Delmonte, A. J.; Haller, J.; Houk, K. N.; Sharpless, K. B.; Singleton, D. A.; Hang, C.; Strassner, T.; Thomas, A. A.; Leung, S. W.; Merrigan, S. R. *Tetrahedron* **2001**, *57*, 5149. (c) Beno, B. R.; Houk, K. N.; Singleton, D. A. *J. Am. Chem. Soc.* **1996**, *118*, 9984.
- (31) Frisch, M. J.; Trucks, G. W.; Schlegel, H. B.; Scuseria, G. E.; Robb, M. A.; Cheeseman, J. R.; Montgomery, J. A., Jr.; Vreven, T.; Kudin, K. N.; Burant, J. C.; Millam, J. M.; Iyengar, S. S.; Tomasi, J.; Barone, V.; Mennucci, B.; Cossi, M.; Scalmani, G.; Rega, N.; Petersson, G. A.; Nakatsuji, H.; Hada, M.; Ehara, M.; Toyota, K.; Fukuda, R.; Hasegawa, J.; Ishida, M.; Nakajima, T.; Honda, Y.; Kitao, O.; Nakai, H.; Klene, M.; Li, X.; Knox, J. E.; Hratchian, H. P.; Cross, J. B.; Adamo, C.; Jaramillo, J.; Gomperts, R.; Stratmann, R. E.; Yazyev, O.; Austin, A. J.; Cammi, R.; Pomelli, C.; Ochterski, J. W.; Ayala, P. Y.; Morokuma, K.; Voth, G. A.;

Salvador, P.; Dannenberg, J. J.; Zakrzewski, V. G.; Dapprich, S.; Daniels, A. D.; Strain, M. C.; Farkas, O.; Malick, D. K.; Rabuck, A. D.; Raghavachari, K.; Foresman, J. B.; Ortiz, J. V.; Cui, Q.; Baboul, A. G.; Clifford, S.; Cioslowski, J.; Stefanov, B. B.; Liu, G.; Liashenko, A.; Piskorz,

P.; Komaromi, I.; Martin, R. L.; Fox, D. J.; Keith, T.; Al-Laham, M. A.; Peng, C. Y.; Nanayakkara, A.; Challacombe, M.; Gill, P. M. W.; Johnson, B.; Chen, W.; Wong, M. W.; Gonzalez, C.; Pople, J. A. *Gaussian 03*, revision C.02; Gaussian, Inc., Wallingford CT, 2004.